Int. J. Solids Structures, 1978, Vol. 14, pp. 81–97. Pergamon Press. Printed in Great Britain

MOVING SINGULARITIES IN ELASTO-DIFFUSIVE SOLIDS WITH APPLICATIONS TO FRACTURE PROPAGATION

MICHAEL P. CLEARY

Department of Mechanical Engineering, Massachusetts Institute of Technology, Cambridge, MA 02139, U.S.A.

(*Received* 1 *March* 1977; *revised* 6 *June* 1977)

Abstract—Solutions are derived for steady-state motion of a singularity class, which includes point sources and dislocations, through a medium in which the elastic stress-field can evolve with time due to the diffusion of an internal second-phase species, such as a pore-fluids and lattice impurity concentrations in a crystalline solid, or the transfer of heat. The technique is to integrate the known influence functions for a stationary singularity. Attention is focused on the most tractable aspect, namely the stress field on the trajectory of motion: this suffices for simulation of growing shear and tensile fractures (e.g. in a porous fluid-saturated solid). Continuous densities of fluid sources and point discontinuities (dislocations) are suitably distributed (as determined by solving the resulting singular integral equations) to satisfy solid stress and fluid pressure or flow conditions on the fracture surfaces. Alternative methods for finding the complete dislocation influence function are discussed and comparisons with existing source solutions are made. Substantial stabilization effects are found in fracture propagation.

INTRODUCTION

The linear theory of fluid-saturated porous media[1] provides a singular example of completely *coupled* elastic deformation and pre-fluid diffusion; the analogous equations of linear coupled thermoelasticity (Chap. 2 of [2]) or of impurity diffusion in a crystalline solid[2] are somewhat less interesting, since the coupling in these is much weaker and is often neglected to facilitate solution extraction. We are, therefore, especially concerned with the porous media application, where the diffusive evolution of the additional "pore-pressure" field variable can induce or be induced by substantial alterations in stress-state; but the other elasto-diffusive media are also covered by our derivations. In particular, we will establish the field of influence in such media for a class of moving singularities which includes point (e.g. fluid) sources, point forces and dislocations. By suitable distribution of sources and dislocations we also extract the behavior around moving shear and tensile faults; analytic estimates[3] of moving shear fault characteristics will be found to compare well with our results. The principal effect might be described as a "drag" on the moving anomaly, a term frequently used in describing crystalline dislocations moving in an impurity atmosphere (although generally accredited to nonlinear effects like stress-dependent diffusivity): the energy dissipation associated with diffusion suggests that an increased force is needed to move the dislocation or crack and this expected impedance is roughly borne out by our results.

Our method is to employ the known solutions[1, 2] for the problem of a singularity which is suddenly introduced at a point in the medium and thereafter (in time) is held fixed in position and strength. The influence function for such a singularity is integrated all along the prospective locus of the corresponding moving singularity: the computations are actually carried out only for the influence on the trajectory of motion since the application to fracture growth does not require the complete influence function. The method can be extended to points off the trajectory but an alternate transform scheme is outlined (Appendix 3) which allows formal convolution with the solution on the trajectory, to cover the whole region of influence. Similar techniques have, occasionally, been employed in the literature (e.g. [8], Section 10.7 and [9] for the study of moving heat sources) and we compare our solutions where relevant (e.g. Appendix 1): the moving dislocation has also been studied[13] but the analysis there makes assumptions about the field which are not applicable here and it seeks special features only, thus there is little correspondence with the present work.

The technique for applying our singularity solutions to simulation of fracture growth is, by now, well established (e.g. [5] for purely elastic application) and Chap. 4 of [2] gives the most general scheme for unsteady motion in a porous medium. The case of steady-state fault motion is the simplest example of time-dependent growth and is simulated by distributing a density of moving dislocations and sources such as to satisfy stress and pore-fluid boundary conditions on the surfaces of the shear or tensile fault. The result is a set of singular integral equations with unknown density and a kernel obtained directly from our singularity influence functions. We describe the matrix equations which result from use of local interpolation functions (like those in [5]) for the density; these have the most general application [2]. However, we choose to solve the equations also by employing Chebyshev polynomials for global interpolation over a somewhat artificial finite crack length, with loads applied near the tip to justify use of our singularity influence functions: the latter method (described in Appendix 2) gave results comparable to those when local interpolation was used and it has substantial advantages (e.g. in incorporating the crack-tip singularity), so in this paper we present its results only. We establish that there is always a zone, sufficiently close to the crack-tip, which is drained. This results in an elevation of the energy supply needed to drive the fracture at increasing speeds: however, at very high speeds, the energy required by the shear fault begins to drop again but that needed by the tensile crack will typically continue to rise, perhaps to as much as an order of magnitude greater than that needed for slow crack growth. There is thus a stabilization of fracture growth which varies somewhat in amount and character from shear to tensile faults.

MOVING SINGULARITIES IN ELASTO-DIFFUSIVE MEDIA

The singularity is considered to have been moving in a straight line at constant velocity V for a long time so that the resulting field depends only on $x - Vt$, where x measures distance along its trajectory from any arbitrary reference point and t is time. For the moment, it will be regarded as a localised distribution $\mu(x - Vt)$ in the vicinity of $x - Vt = 0^-$ (Fig. 1a) and we shall be concerned only with components of its stress-field on the trajectory (i.e. $x_k = 0$); the derivation will be based on the solution for a stationary singularity, $\mu(z, \tau) = H(\tau)\delta(z)$ i.e. one in which a localised μ is introduced, at a point z and time τ, and then kept constant for all remaining time. Although the procedure is formally applicable to a variety of resulting forms for the stress-field, we specifically consider singularities causing stress components at (x, t) which are expressible in the form

$$\sigma(x, t) = (x - z)^n \mathcal{J}[\xi], \quad \xi \equiv (x - z)^2/4c(t - \tau), \tag{1}$$

where n is usually a non-positive integer. The influence function $\mathcal{J}$ will generally contain elastic moduli and diffusion parameters as multiplying constants; the diffusivity of the medium is c (e.g. as defined by *Rice and Cleary* [1]).

It is clear (e.g. see [1, 2]) that the stress due to any singularity distribution $\mu(z, \tau)$ may be

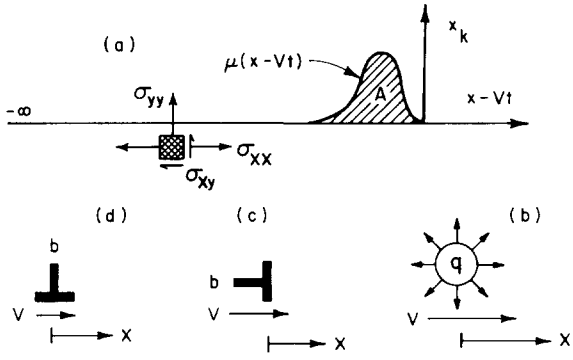

Fig. 1. (a) Moving concentrated anomaly density μ in elasto-diffusive medium. (b) Source in steady-state motion, emitting fluid at constant rate q. (c) "Climbing" edge dislocation, Burger magnitude b. (d) "Gliding" edge dislocation. V is the steady-state velocity.

expressed in terms of the influence function in eqn (1) by means of

$$\sigma(x,t)=\int_{-\infty}^{\infty}\mathrm{d}z(x-z)^n\int_{-\infty}^{t}\mathrm{d}\tau\frac{\partial\mu(z,\tau)}{\partial\tau}\mathscr{J}[\xi]. \tag{2}$$

For the moving distribution $\mu(x-Vt)$ shown in Fig. 1(a), we can pick any generic time and express the field in terms of x: let us pick $t=0$ so that x marks the distance from the head of $\mu(x-Vt)=\mu(x)$. Thus $\mu(z)$ is zero for all $z>0$. The other modification to simplify eqn (2) is to note that we can identify $V\tau$ with a dummy co-ordinate variable z_1, in terms of which $\mu(z,\tau)=\mu(z-V\tau)=\mu(z-z_1)$; the similarity version of eqn (2) is thus

$$\sigma(x)=\int_{-\infty}^{0}\mathrm{d}z(x-z)^n\int_{-\infty}^{0}\mathrm{d}z_1\frac{\partial\mu(z-z_1)}{\partial z_1}\mathscr{J}[\xi],\quad \xi\equiv\frac{V(x-z)^2}{4c(-z_1)}. \tag{3}$$

An integration by parts on the interior integral leads to

$$\sigma(x)=\int_{-\infty}^{0}\mathrm{d}z(x-z)^n\left[\mu(z)\mathscr{J}[\infty]-\left(\frac{V}{4c}\right)\int_{-\infty}^{0}\mathrm{d}z_1\mu(z-z_1)\mathscr{J}'[\xi]\left(\frac{x-z}{z_1}\right)^2\right]. \tag{4}$$

Now we revert to Fig. 1(a) and allow $\mu(z)$ to become arbitrarily closely localised in the vicinity of $z=0^-$, while retaining a constant area A as shown. Then the distribution integrals in eqn (4) are simplified and we deduce

$$\sigma(x)=Ax^n\left\{\mathscr{J}[\infty]-\int_{-\infty}^{0}\mathrm{d}\zeta_1\left(1-\frac{\zeta_1}{\zeta}\right)^{n+2}\left(\frac{\zeta}{\zeta_1}\right)^2\mathscr{J}'[\xi]\right\},\quad \xi\equiv\frac{\zeta^2\left(1-\dfrac{\zeta_1}{\zeta}\right)^2}{\zeta_1}. \tag{5}$$

We have introduced the dimensionless variables $\zeta=Vx/4c$ and $\zeta_1=Vz/4c$. Our last step is to change the integration limits and note the distinction between the cases $\zeta>0$ and $\zeta<0$; we introduce the variable $y=\zeta_1/|\zeta|$ and obtain

$$\sigma(x)=Ax^n\left\{\mathscr{J}[\infty]-|\zeta|\int_0^{\infty}\mathrm{d}y(1\pm y)^{n+2}y^{-2}\mathscr{J}'[\xi]\right\},\quad \xi\equiv\frac{|\zeta|(1\pm y)^2}{y}. \tag{6}$$

The (+) sign applies to $\zeta>0$ while the (−) sign, for $\zeta<0$, will sometimes generate a singular integrand at $y=1$; scrutiny of the derivation shows that the integral is then to be evaluated in the principal value sense. It is sensible that the influence function in eqn (6) should contain only the variable ζ expressing non-dimensional diffusive distance from the singularity. We now show how the result in eqn (6) can be applied to a variety of moving singularities in a typical, and practically most useful, elasto-diffusive medium composed of a solid matrix with fluid-saturated pore-space (as described in [1, 2]).

MOVING FLUID SOURCE IN A POROUS MEDIUM

The first example, illustrating the use of eqn (6), is that of a singularity moving at velocity V which injects fluid at a constant mass rate q per unit length normal to the plane into the medium around it (Fig. 1b). The medium is described by the constitutive equations† of Rice and Cleary[1] and the solution for the stationary source has been given in Chap. 3 of [2]. In the notation of eqn (1), the solutions for the pore-pressure p, on the plane of motion of this infinity long source, and the derivatives in eqn (6) are (with $n=0$ and $A=q$)

$$\mathscr{J}[\xi]=\frac{q}{2\pi\rho_0\kappa}\int_{2\xi^{1/2}}^{\infty}\frac{\mathrm{d}\psi}{\psi}\mathrm{e}^{-\psi^2/4},\quad \mathscr{J}'[\xi]=\frac{-q\,\mathrm{e}^{-\xi}}{4\pi\rho_0\kappa\xi} \tag{7}$$

†The material parameters which enter in [1] are simply shear modulus G, drained and undrained Poisson ratios ν and ν_u, a coefficient measuring undrained pore-pressure $p=-B\sigma_{kk}/3$, and a related coefficient $\eta\equiv 3(\nu_u-\nu)/2B(1+\nu_u)(1-\nu)$.

where κ is the permeability of the medium and ρ_0 is the reference fluid density. If we introduce eqn $(7)_2$ into eqn (6) we readily obtain the solution for the pore-pressure on the plane of motion ((+) sign for $\zeta > 0$)

$$p(\zeta) = \frac{q}{4\pi\rho_0\kappa} \int_0^\infty \frac{dy}{y} e^{-|\zeta|(1\pm y)^2/y}. \tag{8}$$

The solution (eqn 1) and the derivative needed in eqn (6) can also be written for the normal stress (σ) on the plane of motion of the line-source (again derived in Chap. 3 of [2] with $n = 0$):

$$\begin{aligned} \mathcal{J}[\xi] &= \frac{-\eta q}{4\pi\rho_0\kappa} \left[2 \int_{2\xi^{1/2}}^\infty \frac{d\psi}{\psi} e^{-\psi^2/4} \ominus \xi^{-1}(1 - e^{-\xi}) \right]. \\ \mathcal{J}'[\xi] &= \frac{-\eta q}{4\pi\rho_0\kappa} [\ominus \xi^{-1} e^{-\xi} \ominus \xi^{-2}(1 - e^{-\xi}) - \xi^{-1} e^{-\xi}] \end{aligned} \tag{9}$$

Encircled sign options are for σ_{yy} and σ_{xx} respectively (Fig. 1). When eqn $(9)_2$ is used in eqn (6) we deduce (again with (+) sign for $\zeta > 0$)

$$\sigma(\zeta) = \frac{-\eta q}{4\pi\rho_0\kappa} \left[(1 \ominus 1) \int_0^\infty \frac{dy}{y} e^{-\xi} \odot |\zeta|^{-1} \int_0^\infty \frac{dy}{(1 \pm y)^2} (1 - e^{-\xi}) \right], \quad \xi \equiv \frac{|\zeta|(1 \pm y)^2}{y} \tag{10}$$

It is possible to convert the integrals in eqns (8, 10) to known tabulated functions. To do this we write the integral representation [e.g. of Abramowitz and Stegun[4], p. 376] for the modified *Bessel* functions

$$K_\nu(z) = \int_0^\infty dt \cosh(\nu t) e^{-z\cosh t}, \quad z > 0 \tag{11a}$$

and change the variable of integration to $y = e^t$; then the zeroeth and first order *Bessel* functions become

$$K_0(z) = \frac{1}{2} \int_0^\infty \frac{dy}{y} e^{-(z/2)(y+[1/y])}, \quad K_1(z) = \frac{1}{4} \int_0^\infty \frac{dy}{y} \left(y + \frac{1}{y} \right) e^{-(z/2)(y+[1/y])} \tag{11b}$$

Now it is obvious that eqn (8) can be rewritten as

$$p(\zeta) = \frac{q}{2\pi\rho_0\kappa} e^{-2\zeta} K_0(2\zeta). \tag{12}$$

We need to manipulate eqn (10) a little before comparing to known integrals. It is easiest to reduce eqn (10) for $\zeta > 0$ so let us consider that case for demonstration of the technique.

In deference to eqns (8, 12), eqn (10) may be written

$$\sigma(\zeta) = \frac{-\eta q}{4\pi\rho_0\kappa} \{ e^{-2\zeta} [2K_0(2\zeta) \ominus I(\zeta)] \ominus |\zeta|^{-1} \} \tag{13a}$$

where the integral $I(\zeta)$ takes the form

$$I(\zeta) = \int_0^\infty \frac{dy}{y} \left(\frac{y}{|\zeta|(1+y)^2} + 1 \right) e^{-|\zeta|(y+[1/y])} = \int_0^\infty \frac{dy}{y^2} e^{-|\zeta|(y+[1/y])} \tag{13b}$$

Here we have performed an integration by parts on the first integral. By noting the symmetry in the definition of $K_1(z)$ we recognise that $I(\zeta) = 2K_1(2\zeta)$ so that eqn (10) has the tabulated representation

$$\sigma(\zeta) = \frac{-\eta q}{2\pi\rho_0\kappa} \{ e^{-2\zeta} [K_0(2\zeta) \ominus K_1(2\zeta)] \ominus (2\zeta)^{-1} \} = \begin{Bmatrix} \sigma_{yy} \\ \sigma_{xx} \end{Bmatrix}. \tag{13c}$$

This can be shown to be valid also for $\zeta < 0$, by taking a little care with the principal value integrals. Now there actually is another means for determining the whole influence field of the moving source: we give the method in Appendix 1 and show that eqns (12), (13c) are the correct solutions for the pore-pressure and normal stress on the plane of motion of the source. Such alternate solutions are usually not available, however, so we have to employ eqn (6) exclusively. Such is the case for the moving dislocations considered next: for these, eqn (6) serves both to determine the influence field on the trajectory of motion and through this, as input to a formal scheme outlined in Appendix 3, to establish the complete influence function.

MOVING DISLOCATIONS IN A FLUID-SATURATED POROUS MEDIUM

A discussion on the use of stationary dislocations to simulate faulting of an elastic medium has been given by Cleary[5]. Our purpose here is to use long straight† edge dislocations to simulate a moving fault in a diffusive medium. We have need of the solutions for two orthogonal orientations of the slip direction: these are shown in Fig. 1(c, d) and will be referred to as the "gliding" (Fig. 1d) and "climbing" dislocations. Toward these, we shall use the solutions in eqn (47) of [1], derived for a suddenly introduced stationary dislocation, to write eqn (1) and then extend the solutions to a moving dislocation by means of eqn (6). For the "gliding" dislocation we find that the pore-pressure and normal stress on its plane of motion is zero while the shear-stress is given by $A \equiv b$, $n = -1$ (in eqn (1)) and

$$\mathscr{J}[\xi] = \frac{Gb}{2\pi(1-\nu_u)}\left[1 - \left(\frac{\nu_u - \nu}{1-\nu}\right)\xi^{-1}(1-\mathrm{e}^{-\xi})\right] \tag{14a}$$

$$\mathscr{J}'[\xi] = \frac{Gb(\nu_u - \nu)}{2\pi(1-\nu_u)(1-\nu)}[\xi^{-2}(1-\mathrm{e}^{-\xi}) - \xi^{-1}\mathrm{e}^{-\xi}]. \tag{14b}$$

We insert eqn (14b) in eqn (10) to obtain the shear-stress $\tau(x)$ on the plane of motion

$$\tau(x) = \frac{Gb}{2\pi(1-\nu_u)x}\left\{1 - \left(\frac{\nu_u - \nu}{1-\nu}\right)\left[|\zeta|^{-1}\int_0^\infty \frac{\mathrm{d}y(1-\mathrm{e}^{-\xi})}{(1\pm y)^3} - \int_0^\infty \frac{\mathrm{d}y\,\mathrm{e}^{-\xi}}{(1\pm y)y}\right]\right\} \tag{14c}$$

where $\xi \equiv |\zeta|(1\pm y)^2/y$ as before and (+) sign applies to $\zeta > 0$. We did not succeed in writing the integrals of eqn (14c) in terms of tabulated functions but rather resorted to a numerical evaluation of them: of course, once computed, they constitute integral representations of the resulting function and we were satisfied to regard them as such. Thus, we denote the pair of integrals in square parentheses as

$$g_1(\zeta) \equiv |\zeta|^{-1}\int_0^\infty \frac{\mathrm{d}y(1-\mathrm{e}^{-\xi})}{(1\pm y)^3} - \int_0^\infty \frac{\mathrm{d}y\,\mathrm{e}^{-\xi}}{(1\pm y)y}, \quad \xi \equiv \frac{|\zeta|(1\pm y)^2}{y} \tag{15}$$

and a plot of $g_1(x)$ is shown in Fig. 2(a). It is important to note the asymmetry of $g_1(x)$ with respect to $x = 0$. This can actually be identified as the cause of a drag force on the dislocation, a phenomenon not previously considered in the literature on crystalline dislocations.

For the "climbing" dislocation, there is a pore-pressure induced on the plane of motion (Fig. 1c); the stationary solution has $n = -1$ and influence functions (eqns (1), (6)) are

$$\mathscr{J}[\xi] = \frac{-Gb}{2\pi(1-\nu_u)}\left[\frac{2B(1+\nu_u)}{3} - \left(\frac{\nu_u - \nu}{1-\nu}\right)\eta^{-1}\mathrm{e}^{-\xi}\right] \tag{16a}$$

$$\mathscr{J}'[\xi] = \frac{-Gb(\nu_u - \nu)}{2\pi(1-\nu_u)(1-\nu)}\eta^{-1}\mathrm{e}^{-\xi} \tag{16b}$$

Insertion of eqn (16b) into eqn (6) gives the pore-pressure $p(x)$ on the plane of motion (at

†These are dislocations which produce a "plane strain" deformation state.

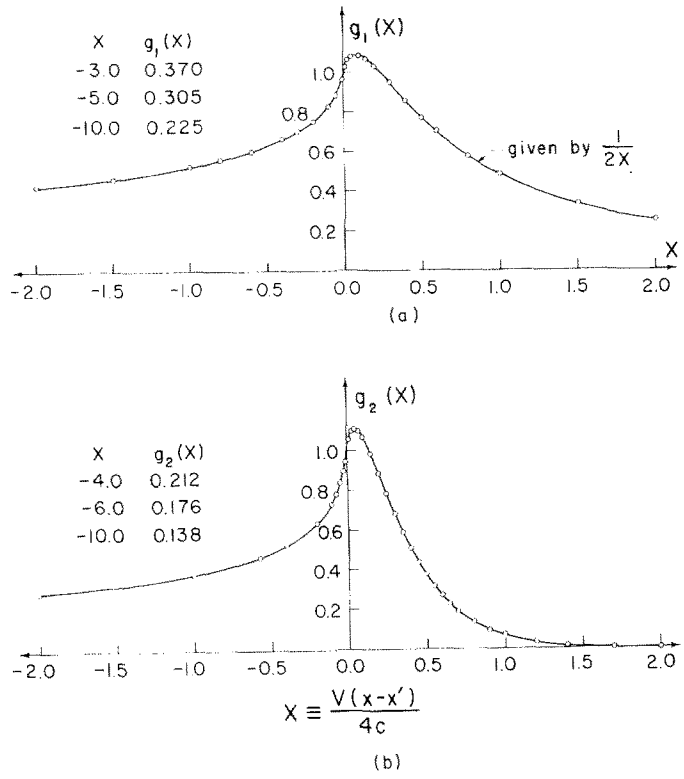

Fig. 2. (a) Influence function for shear stress on plane of "gliding" dislocation. (b) Additional influence function needed for pore-fluid pressure and normal stress on plane of "climbing" dislocation (medium diffusivity c).

distance x from the dislocation)

$$p(x) = \frac{-Gb}{2\pi(1-\nu_u)x}\left\{\frac{2B(1+\nu_u)}{3} - \eta^{-1}\left(\frac{\nu_u-\nu}{1-\nu}\right)g_2(\zeta)\right\} \tag{16c}$$

where we have used the notation

$$g_2(\zeta) = |\zeta|\int_0^\infty \frac{dy(1\pm y)}{y^2}e^{-\xi}, \quad \xi \equiv \frac{|\zeta|(1\pm y)^2}{y} \tag{17}$$

Again, $g_2(X)$ is a function which can be computed numerically (with (+) sign for $X>0$) and it is shown in Fig. 2(b).

We will also have use for the normal stress $\sigma(x)$ on the plane of motion of the "climbing" dislocation. The stationary solution (eqn (1)) is given by $n=-1$ and

$$\mathcal{J}[\xi] = \frac{Gb}{2\pi(1-\nu_u)}\left[1-\left(\frac{\nu_u-\nu}{1-\nu}\right)(2e^{-\xi}+\xi^{-1}(1-e^{-\xi}))\right] \tag{18a}$$

$$\mathcal{J}'[\xi] = \frac{Gb(\nu_u-\nu)}{2\pi(1-\nu_u)(1-\nu)}[2e^{-\xi}-\xi^{-2}(1-e^{-\xi})+\xi^{-1}e^{-\xi}]. \tag{18b}$$

Now eqn (6), after eqn (18b) is inserted for $\mathcal{J}'[\xi]$, reduces to

$$\sigma(x) = \frac{Gb}{2\pi(1-\nu_u)x}\left\{1-\left(\frac{\nu_u-\nu}{1-\nu}\right)[2g_2(\zeta)-g_1(\zeta)]\right\} \tag{19}$$

We now have, in eqns (12), (13c), (14c), (16c), (19), all of the solutions which we need to

simulate a shear or tensile fault, moving through a porous medium under steady-state conditions, with arbitrary accompanying slip, dilation and opening displacement. We note that we could derive many additional solutions, such as those for moving body-forces (acting on solid or fluid) or three-dimensional slip and dilation as derived for the stationary problem in Chap. 3 of [2]. We shall make only limited use here even of the source and dislocation solutions just derived, so we defer such exhaustive analyses to another time. The method for deriving the stress-field on the plane of motion is now clear enough and we shall next consider the usefulness, even of this apparently limited knowledge of the singular influence function,† toward solving fracture problems where the boundary conditions are specified on the fracture plane.

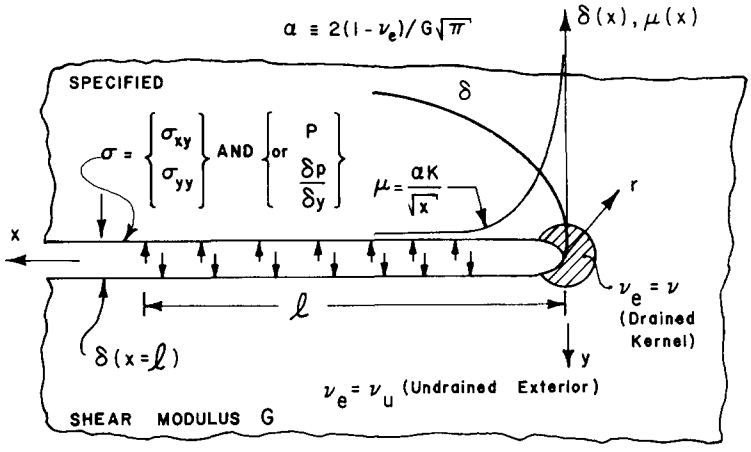

Fig. 3. Near-tip region of a semi-infinite shear or tensile brittle fault in a fluid-saturated porous medium. Loadings are applied over a length l near the tip ($x = 0$). Stress field is singular as radius $r \to 0$ and there results a drained kernel (with effective Poisson ratio $\nu_e \simeq \nu$) for sufficiently small r, even though the exterior region is effectively undrained ($\nu_e \simeq \nu_u$). Sliding or opening discontinuity is $\delta(x)$ and its derivative $\mu(x)$, the dislocation density, is singular as $x \to 0$.

APPLICATION TO SIMULATION OF MOVING SHEAR AND TENSILE FAULTS

We limit ourselves to faults (Fig. 3) on which either shear or normal stress, pore-pressure or rate of fluid loss to formation (normal derivative of p) are specified. We simply distribute either "gliding" or "climbing" dislocations and moving fluid sources in such a fashion as to satisfy both traction and fluid conditions on the faces of the fault (see Chap. 4 of [2] for details in the general case). Let $\mu(x)$ represent the distributed density of moving dislocations and $\theta(x)$ the density of fluid sources with constant suction rate: let x measure the distance from the fault tip, in the co-ordinate system moving at constant velocity V with the tip. Let $\sigma^D(x-z)$, $p^D(x-z)$ denote the stress (shear or normal) and pore-pressure at a point x due to a moving dislocation at z while $\sigma^s(x-z)$, $p^s(x-z)$ denote those due to a moving source. These will be extracted from eqns (12)–(19) as they are needed. Suppose we use $\sigma(x)$ and $p(x)$ to denote the values of stress and pore-pressure (or, in unlikely context, its normal derivative) on the line of the fault (these may be given or may be coupled to $\mu(x)$ and $\theta(x)$); then we get the integral equations

$$\sigma(x) = \int_{-\infty}^{0} \mu(z)\sigma^D(x-z)\,dz + \int_{-\infty}^{0} \theta(z)\sigma^s(x-z)\,dz$$

$$p(x) = \int_{-\infty}^{0} \mu(z)p^D(x-z)\,dz + \int_{-\infty}^{0} \theta(z)p^s(x-z)\,dz \qquad (20)$$

For simplicity, we assume that the fault stretches to $x = -\infty$ from its tip at $x=0$, so that use of our moving singularity solutions is physically rigorous.‡

†A method for obtaining the complete influence function is outlined in Appendix 3: the task is greatly simplified by knowing the value of stress on the trajectory.

‡However, finite faults with somewhat artificial histories can also be simulated, in an obvious fashion.

By inspecting the solutions for moving sources and dislocations, given in the foregoing section, we observe that σ^D and p^D are singular as $(x-z)^{-1}$ whereas σ^s and p^s are singular only as $\ln(x-z)$. We have already solved a variety of singular integral equations containing an $(x\text{-}z)^{-1}$ in the kernel (e.g. see [5]) and there have been a number of workers on the numerical solutions of integral equations with a $\ln(x-z)$ kernel, as they arise in smooth torsion geometries, for instance (e.g. [6], Chap. 5). Coupled singular integral equations, all with $(x-z)^{-1}$ singularity kernels, have been solved in applying the boundary integral equation method to elastic fracture problems (e.g. Chap. 4 in [6]). However, there appears (e.g. [7]) to be little general experience with coupled equations of the kind in eqn (20); still, we can follow the usual [5] procedures and write

$$\mu(x) = \sum_{k=1}^{N} \mu_k m_k(x), \quad \theta(x) = \sum_{k=1}^{M} \theta_k s_k(x) \tag{21}$$

where $m_k(x)$ and $s_k(x)$ are suitable interpolation functions (local or global) and N is generally larger than M (unless, for instance, the filtration of fluid from the fault opening into the surrounding medium has a dominant influence†).

The idea is that $\sigma(x)$ and $p(x)$ will be imposed at a discrete number of points, i.e. represented by their values $\sigma_k (k = 1, \ldots, N)$ and $p_j (j = 1, \ldots, M)$ at discrete nodal points. Then eqns (24) transform to an overall matrix equation

$$\begin{Bmatrix} \sigma_k \\ p_j \end{Bmatrix} = \begin{bmatrix} \xi_{km} & \phi_{kn} \\ \chi_{jm} & \psi_{jn} \end{bmatrix} \begin{Bmatrix} \mu_m \\ \theta_n \end{Bmatrix}, \quad \begin{matrix} k, m = 1, \ldots, N \\ j, n = 1, \ldots, M. \end{matrix} \tag{22a}$$

The submatrix elements are composed in a standard fashion, namely

$$\xi_{ij} = \int_{-\infty}^{0} \sigma^D(x_i - z) m_j(z)\, \mathrm{d}z, \quad \chi_{ij} = \int_{-\infty}^{0} p^D(x_i - z) m_j(z)\, \mathrm{d}z$$

$$\phi_{ij} = \int_{-\infty}^{0} \sigma^s(x_i - z) s_j(z)\, \mathrm{d}z, \quad \psi_{ij} = \int_{-\infty}^{0} p^s(x_i - z) s_j(z)\, \mathrm{d}z \tag{22b}$$

but the interpolation functions should, of course, be chosen to give well-conditioned matrices upon integration with the singular influence functions; a very simple set of localised functions with exactly this property have been employed by Cleary [5], and they are valid for any fault domain.

Alternately, we may regard eqns (24) as the limiting form of equations governing a symmetrically spreading finite fault when we apply loadings very near to the tip only; then there happens to be a simple way of computing the submatrices without (remarkably) any specific reference to the interpolation functions. This is achieved by choosing the functions to be Chebyshev polynomials. The method is detailed in Appendix 2. Essentially, the known stresses $\sigma(x)$ and $p(x)$ are imposed at zero points of the Chebyshev polynomials of the second kind while the densities are computed at zero points for polynomials of the first kind.

The Chebyshev scheme exploits the known $x^{-1/2}$ singularity (Fig. 3) in the density $\mu(x)$ near the fault-tip ($x = 0$) and is extremely convenient in determining the strength of that singularity; thus we chose to use it for our preliminary investigations, mainly to gain some experience with alternatives to the scheme implied by eqns (22b). It happens to be amenable also (as explained in Appendix 2) to problems where the fault closes smoothly [say $\mu(x) \sim x^{1/2}$ in Fig. 2] so we employ it exclusively in this paper. Nevertheless, we emphasize that the infinite fault problem with smooth closure lends itself best to schemes like those in [5] and (22b), especially as to inclusion of the source density $\theta(x)$: unlike $\mu(x)$, this does not have a well-known singularity as $x \to 0$ but is limited by the requirement that it produce a bounded jump in p across $x = 0$.

The coupled eqns (20), (22) merit a much lengthier treatment than we can give here so we

†Example of this special case is fluid loss to the formation from an extensive fracture (e.g. [2]), produced by hydraulic underground pressurisation.

shall hereafter specialize to the class of problems where there is no need for the source density $\theta(x)$. Further, we shall give only the results of employing the Chebyshev polynomial interpolation on a finite fault length; the infinite fault results will be extracted† by imposing tractions over a sufficiently small near-tip region of the finite fault. The reduced version of eqns (20) will then take the form (adopting the half-fault length as unit dimension)

$$\sigma(x) = C\int_{-1}^{+1} \mu(z)[(x-z)^{-1} + k(x-z)]\,dz \tag{23}$$

where C contains material moduli and $k(x-z)$ is a bounded displacement kernel for all of the problems considered in this paper. The stress $\sigma(x)$ may be a shear stress or a normal stress on the fault line and thus $\mu(z)$ is a density of either "gliding" (sliding) or "climbing" (opening) dislocations. The pore-pressure or rate of fluid flow across the fault is to be accepted as whatever eqn $(20)_2$ implies with $\theta(z) = 0$.

The scheme for solving eqn (23) numerically is in Appendix 2. We first change the unknown variable to $F(z)$, as given by

$$\mu(z) = F(z)/\sqrt{(1-z^2)} \tag{24a}$$

and immediately recognise that $F(z = \pm 1.0)$ measures the strength of the singularity, frequently defined (Fig. 3) in terms of the "stress-intensity factor" K. Thus, for shear or tensile faults, the intensity of the singularity is given by

$$F(z = \pm 1.0) = 2(1-\nu)K/G\sqrt{\pi} \tag{24b}$$

because, as we have noted already, there is always a drained zone sufficiently close to the tip.‡ Thus $F(\pm 1.0)$ will henceforth be used to calibrate the change in K with increasing speeds of fault propagation.

The numerical version of eqn (23) now takes the form (see details in Appendix 2)

$$\sum_{k=1}^{2M} [(t_k - x_r)^{-1} - k(x_r - t_k)]F(t_k) = -2M\sigma(x_r)/\pi C, \quad r = 1, \ldots, 2M-1$$

$$\sum_{k=1}^{2M} F(t_k) = 0; \; t_k = \cos\frac{\pi(2k-1)}{4M}, \quad x_r = \cos\frac{\pi r}{2M}. \tag{25}$$

The last condition on the $F(t_k)$ is arbitrarily imposed to exclude any net entrapped dislocation in the fault and t_k, x_r are the zero points of the first and second kind (respectively) of Chebyshev polynomials. Equation (25) allows an arbitrary stress distribution on the fault but we are exclusively interested in a fault spreading symmetrically with respect to its initiation point§ (i.e. symmetric about $x \simeq 0$ in Fig. 4) so we further impose

$$F(t_{M+1-k}) = -F(t_k), \quad \sigma(x_{M-r}) = \sigma(x_r). \tag{26a}$$

Now the matrix equation corresponding to eqns (22) simplifies to

$$\sum_{k=1}^{M} \{(t_k - x_r)^{-1} - (t_{2M+1-k} - x_r)^{-1} - k(x_r - t_k) - k(x_r - t_{2M+1-k})\}F(t_k)$$

$$= -2M\sigma(x_r)/\pi C, \quad r = 1, \ldots, M. \tag{26b}$$

†These were checked against results obtained directly by using the interpolation functions of Cleary [5] for $\mu_k(x)$ in eqns (21), (22).

‡This characteristic has also been proved and elaborated upon in recent analytical work [3, 12].

§Note that the precise physical interpretation of the problem being modelled involves a pair of dislocation densities, one having come from $X \simeq -\infty$ and the other (a negative image of the first about the midpoint between their heads) having propagated from $X = +\infty$.

The correction terms containing t_{2M+1-k} are interference terms from the other side of the fault and are important when the driving stresses are distributed over the whole fault length; however, when the loaded length l (Fig. 4) is very small ($l/a \leq 0.2$ was found appropriate) then $F(z)$ decays very rapidly with distance from the tip, and, when $(x_r - t_{2M+1-k})$ is comparable to $(x_r - t_k)$, the multiple $F(t_k)$ is negligible. Thus we can effectively simulate a semi-infinite propagating fault. The results compare perfectly with other solutions of eqns (26), obtained by using the localised interpolation functions described in [5]: there was actually no appreciable numerical advantage to either method in simulating the smoothly closing semi-infinite fault but the ability to extract K so readily favored by *Chebyshev* scheme (since the $x^{-1/2}$ singularlity is awkward to incorporate with local interpolation): consequently, we present only solutions to eqns (26b) in our sample results of the next section.

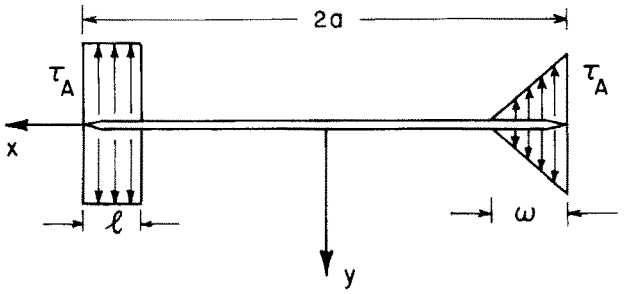

Fig. 4. Schematic of a finite internal fault with two kinds of symmetric loading applied, very near to the tips only: "driving" forces are shown on the left as uniform stress τ_A over length $l \ll a$ while "cohesive" forces are modelled (on the right) as linearly decreasing from τ_A over length $\omega(\omega \ll a)$. The spreading finite fracture can thus be approximated by using our moving singularity distributions and resulting equations are amenable to Chebyshev interpolation.

SAMPLE RESULTS FOR MOVING FRACTURES IN POROUS MEDIA

We present here just two specific kinds of results, applicable to both shear and tensile faults. The first is a plot of the function $F(x)$ for various velocities of motion of the fault V: although the method is physically rigorous only for near-tip loading on a finite fault, the characteristics of the latter are well captured by the results for uniform loading over the fault length and we have decided to present these results for their transparency of interpretation. Thus, $\sigma(x_r)$ are all set equal to τ_A in eqn (26b) and the results for $F(t_k)$ are to be compared with the known analytic solution for an elastic response (involving effective Poisson ratio, ν_e), $F(z) = \mu(z)\sqrt{(1-z^2)} = 2\tau_A z(1-\nu_e)/G$; specifically, for $V \to \infty$ or $V \to 0$, the solution for $F(z)$ is known with $\nu_e \equiv \nu_u$ or $\nu_e \equiv \nu$, respectively.

Since the loading is applied over a length l (in this case $l = a \equiv 1.0$), the appropriate dimensionless measure of velocity is $Vl/4c$. When this parameter is very small, the solution for $F(t_k)$ should agree with the drained elastic solution ($\nu_e \equiv \nu$) and this was found to be the case, as shown in Fig. 5(a). As $Vl/4c$ increases, the solution for $F(t_k)$ should, in some sense, tend toward the undrained elastic solution ($\nu_e \equiv \nu_u$), which it should reach when $Vl/4c \to \infty$; this is exactly what happens in Fig. 5(a) but we note the central point that the slope of $F(z)$ near the tip ($z = 1.0$) always remains at its drained value α, and goes over to the undrained value α/β in a transition region with size decreasing as $Vl/4c$ increases. *Thus, there is always a region (however small), near the tip of a shear or tensile crack, which is drained.* Only the numerical values of $Vl/4c$, required for a given amount of transition between drained and undrained, distinguish between shear and tensile faults. Physically, it is clear that drainage takes place across the fault surface in the antisymmetric shearing case but that symmetry demands a zero pore-pressure gradient (and hence no fluid flow) across a tensile fault surface, thereby causing a much slower process than in the shear case: this is precisely what we found and it is closely accurate to say that the results for $Vl/4c \simeq 0.5$ in the tensile problem are the same as those for $Vl/4c \simeq 5.0$ in the shear problem (thus we have so represented them, for brevity, in Fig. 5(a)).

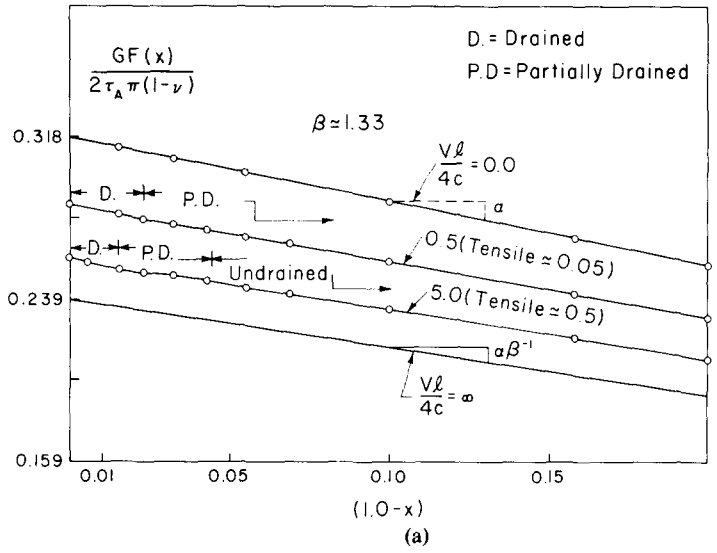

(a)

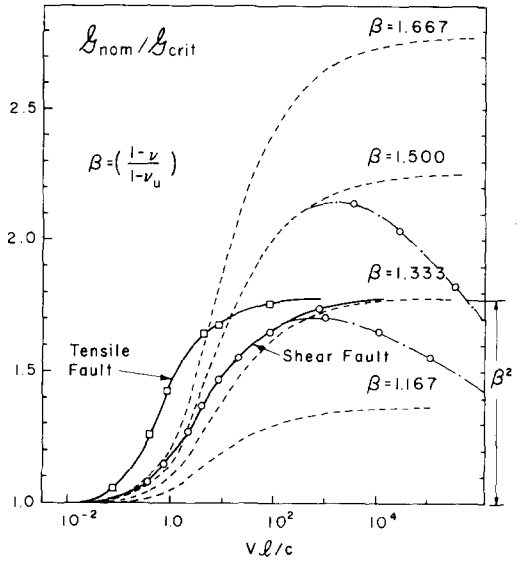

(b)

Fig. 5. (a) Solutions for dislocation density, $F(z) = \mu(z)\sqrt{(1-z^2)}$ at various velocities V. Fault is uniformly loaded ($l = a, \omega = 0$ in Fig. 4) so as to facilitate observation of drained to undrained transition in μ; near-tip zone is always drained. (b) Driving stresses (symmetric about $x = 0$ in Fig. 4) in terms of their energy release rate $\mathcal{G}_{\text{nom}}$, needed to keep a fault propagating at any specific velocity. Dashed lines are for uniform τ_A over length $l \simeq 0.191a$ near the tip (left side of Fig. 4); connected numerical symbols are for positive τ_A over length $\omega \simeq 0.191a$ (right side of Fig. 4). Chain-link results are shown for the case where $\mathcal{G}$ due to uniform τ_A over $l \simeq 0.191a$ (left side of Fig. 4) must exactly cancel that due to negative constant cohesive stresses over $\omega \simeq 0.02l$ (right side of Fig. 4).

The second kind of result is related to the concept of a "fracture criterion" for propagation of the shear or tensile fault. The simplest such criterion is that the "stress-intensity" factor $K = K(\tau_A, Vl/4c)$ must be kept at a critical value (say K_{nom}) to maintain propagation: most feasibly this K_{nom} would be measured for completely drained spreading ($Vl/4c \to 0$), and we suppose it could be produced by a stress distribution τ_A^{nom} under such conditions. We now ask what stresses (as calibrated by some appropriate norm, τ_A, of a specified distribution) are needed to produce the same K_{nom} under conditions where $Vl/4c$ is not negligible. Clearly the answer is that $\tau_A/\tau_A^{\text{nom}}$ is the same as $K(Vl/4c \simeq 0)/K$ and the latter is simply given, in our present scheme, by $F(Vl/4c \simeq 0)/F(Vl/4c)$, where F is the magnitude of $F(z)$ at the tip of the fault. However, instead of plotting the ratio directly we choose to show its square $(\tau_A/\tau_A^{\text{nom}})^2$, which we call $\mathcal{G}_{\text{nom}}/\mathcal{G}_{\text{crit}}$, in Fig. 5(b); the terminology is deliberate because $\mathcal{G}$ is conventionally

used for the "energy release rate" in fracture mechanics and $(\tau_A/\tau_A^{nom})^2$ is none other than the ratio of energies which τ_A and τ^{nom} could supply under completely drained brittle facture conditions. The results shown by dashed lines in Fig. 5(b) are taken from analytic computations in [3]; we show our results only for $\beta \equiv (1-\nu)/(1-\nu_u) = 4/3$, since a similar relation to the analytic results pertained for all other values of β. There does appear to be a consistently earlier rise for the $\mathcal{G}$ vs V curve which we obtain than for that given in [3], especially when we account for the shorter effective length of our triangular distribution of driving stress (right of Fig. 4) as against their constant τ_A (left of Fig. 4).

Details of computation: (a) *shear fault*

The density $\mu(z)$ in eqn (23) is a distribution of "gliding" dislocations and the stress $\sigma(x)$ is the shear stress on the fault surface so eqns (14c), (15) give us $C = G/2\pi(1-\nu)$ and the modifying kernel function turns out to be

$$k(x-z) = \left(\frac{\nu_u - \nu}{1-\nu_u}\right)\left(\frac{V}{4c}\right)\left[\frac{1-g_1(X)}{X}\right], \quad X \equiv \frac{V(x-z)}{4c}. \tag{27}$$

This function is bounded provided the first derivative of $g_1(X)$ is bounded at $X = 0$ (as in Fig. 2(a)), so that the matrix equivalent (eqn (26b)) of eqn (23) can be rigorously derived. It was then straight-forward to compute the matrix multipling $F(t_k)$ in eqn (26b), for any desired velocity parameter $V/4c$ (all distances being scaled to the unit half length a in Fig. 2). Finally, any desired stress distribution $\sigma(x_r)$ could be imposed and the solution for $F(t_k)$ obtained by standard linear algebra routine: in particular, we use constant stresses $\sigma(x_r) = \tau_A$ for Fig. 5(a) and $\sigma(x_r)$ linearly decreasing, with distance from the crack-tip, to zero at (and outside) $l \simeq 0.191a$ for Fig. 5(b). Many other circumstances were tested (as reported in Chap. 5 of [2]) and would require extensive physical explanations but we just mention the case where fixed negative "cohesive" stresses were distributed over a length $\omega \ll l$ (linearly decreasing from the tip), together with positive ("driving") stresses, uniformly τ_A over a length $l(\ll a)$: the magnitude of the stress τ_A was chosen so that the K values they produced (at any $Vl/4c$) just cancelled each other and $(\tau_A/\tau_A^{nom})^2$ was plotted for the driving stresses $(\tau_A^{nom}$ again corresponding to $Vl/4C \simeq 0)$. Naturally, it exhibits the same rising behavior as before, as long as $V\omega/4c$ is negligible (while $Vl/4c$ is not); however, eventually the fault moves so fast that drainage cannot take place even on the scale of ω and the "cohesive" stresses begin to exert a smaller K. At this stage the curve begins to drop again, e.g. as shown by the chain-link curve in Fig. 5(b) for the particular case $\beta \simeq 4/3$ and $\omega/l \simeq 0.02$; it drops from β^2 to β (approx), in agreement with our physical reasoning (Chap. 5 of [2]). A corresponding effect is found, under identical circumstances, for the tensile fault (so we omit the plot thereof): it would mean that faults in porous media exhibit an instability, the stresses required to drive them at intermediate velocities being greater than those needed at somewhat higher velocities. This point is further elaborated for shear faults in [3] but we have found (Chap. 5 of [2]), by the present method, a further remarkable source of stabilization for tensile faults. This would remove the instability and make the curve of $\mathcal{G}_{nom}/\mathcal{G}_{crit}$ in Fig. 5(b) rise always, to $3(1-\nu)/(1-\nu_u)[3-2B(1+\nu_u)]$ at $V\omega/4c \to \infty$; formally, it could thus rise indefinitely if $B \simeq 1.0$, $\nu_u \simeq 0.5$ (the case often assumed for clayey soils). In other words, it would be increasingly difficult (to degrees determined by ν_u, ν, B) to make a tensile crack propagate more rapidly (as calibrated by the dimensionless parameter $V\omega/4c$) through a fluid-saturated porous medium, reasonably assuming that such velocities are not in the dynamic range.† It would be impossible in the case where fluid and solid constituents have a much lower compressibility than the structural matrix of the medium (corresponding to $B \simeq 1.0$ and $\nu_u \simeq 0.5$ above). Thus, it should be very difficult to induce rapid fracture in various materials when they are saturated: this result appears to be strongly supported by physical observations on tensile rupture of rock, ice and biological tissue.

†The parameter $\rho V^2/G$ (where ρ is material density), roughly determining the ratio of kinetic energy to strain energy, is usually negligible for $V\omega/4c$ of order unity (where ω is readily estimated from microstructurally based "crack-tip opening displacement" $\delta(\omega)$ or analogous measures [2]).

(b) *Tensile fault*

The density $\mu(z)$ in eqn (23) is now a distribution of "climbing" dislocations and the stress $\sigma(x)$ is the normal stress on the crack surface so that eqn (19) gives $C = G/2\pi(1-\nu)$ and the variable kernel function

$$k(x-z) = \left(\frac{\nu_u - \nu}{1-\nu_u}\right)\left(\frac{V}{4cX}\right)[(2-\alpha(x))(1-g_2(X)) - (1-g_1(X))] \tag{28}$$

where $\alpha(x)$ is zero for our present purposes.† Here the singularity in $k(x-z)$ depends on that of $g_1'(X)$ and $g_2'(X)$ at $X = 0$ (as determined by Figs. 2(a, b)) so it is appropriately well-behaved for the derivation of the matrix equivalent eqns (26b). The remaining steps follow exactly on those for the shear fault and the results (e.g. Figs. 5(a, b)) correspond except for the translated dependence on $Vl/4c$ caused by slower drainage behavior. However, we note that we have not used a source distribution $\theta(z)$ at all: this was not needed in the shear problem because $p \simeq 0$ was satisfied (by antisymmetry) on the fault line but $\theta(z) = 0$ on the tensile crack surface implies *no penetration of fluid through the walls* of the surrounding medium. There are many problems where this is not an adequate model (e.g. gas penetration and cracking after an underground explosion) and even the presence of dilatancy in the shear fault requires a distribution of $\theta(z)$: inclusion of $\theta(z)$ requires a treatment of the logarithmic kernel which arises in eqns (12), (13c) so we defer such consideration to a more extensive paper on practical applications.

CONCLUSIONS

We have been able to establish sufficient information about the field of influence of singularities in steady-state motion, specifically moving sources and dislocations, in an elasto-diffusive medium such as a fluid-saturated porous solid, that the simulation of shear and tensile fracturing can be performed and useful practical information extracted. We did not aim to extract the complete influence function, although that is attained for the moving fluid source (Appendix 1), partly because we did not initially require the stress field off the fracture surface. However, we must next turn our attention to just that question, on which only a little analytical progress has been made[3, 12]; progress on the exterior field will require a more extensive description of the solution for mobile dislocations. It is possible to extend the field off the dislocation trajectory by (numerically) performing the inversions of the Fourier transforms established in Appendix 3; some features can also be extracted by applying our method of integration to the stationary influence function in a manner analogous to Section 10.7 of [8]. These problems are not yet resolved and we propose them as the next in a series of steps to further advance the method of using singularity distributions (including, perhaps, unsteady motion and nearby free surfaces) for the analysis of fracture growth in shear or tensile modes, with various amounts of shear dilation or with combinations of fluid boundary conditions. The results just presented are, therefore, just a first stage in applying the general method of point anomaly distribution (described in Chap. 4 of [2]) to simulate localized rupture in (e.g. porous) time-dependent media.

Acknowledgements—The work was performed under the support of Grant No. GA-43380 from the National Science Foundation to Brown University. Helpful interaction with J. R. Rice, D. A. Simons and J. W. Rudnicki is gratefully acknowledged.

REFERENCES

1. J. R. Rice and M. P. Cleary, Some basic stress diffusion solutions for fluid-saturated elastic porous media with compressible constituents. *Rev. Geophs. Space Physics* **14**, 227–241 (1976).
2. M. P. Cleary, Fundamental solutions for fluid-saturated porous media and application to localized rupture phenomena. Thesis in partial fulfilment of Ph.D requirements, Brown University, Rep. No. GA-43380 to NSF, 1975. Chap. 3 in *Int. J. Solids Structures* **13**, 785–806 (1977).

†Actually, when inserting the second zone ω in the tensile crack problem (by analogy with our description for the shear fault) we defined the "cohesive" stresses to be $\sigma + p$ (in accordance with an "effective stress" law) and so obtained a different kernel inside ω from that outside, according to the definition $\alpha(x) = 0$ for $|x| \leq a - \omega$ and $\alpha(x) = \eta^{-1}$ for $a \geq |x| \geq a - \omega$. It was the insertion of this effective stress criterion for the decohesion process which gave rise to the substantial stabilization of tensile cracks in porous media, as mentioned earlier.

3. J. R. Rice and D. A. Simons, The stabilization of spreading shear faults by coupled deformation-diffusion effects in fluid-infiltrated porous materials. *J. Geophys. Res.* **81**(29), 5322–5334 (1976).
4. M. Abramowitz and I. A. Stegun, *Handbook of Mathematical Functions*. Dover, New York (1965).
5. M. P. Cleary, Continuously-distributed dislocation model for shear-bands in geological materials. *Int. J. Num. Methods in Eng.*, **10**, 679–702 (1976).
6. T. A. Cruse and F. Rizzo, Boundary integral equation method: computational applications in applied mechanics. *Proc. ASME Summer Conference on Appl. Mech.* RPI, Troy, New York (1975).
7. V. V. Ivanov, *The Theory of Approximate Methods and their Application to the Numerical Solution of Singular Integral Equations* (Trans. from Russian by A. Ideh, Editor R. S. Anderson), Noordhoff, Leydn (1976).
8. H. S. Carslaw and J. C. Jaegar, *Conduction of Heat in Solids*. 2nd Edn. Oxford University Press (1959).
9. W. Nowacki, *Thermoelasticity*. Pergamon Press and PWN, Warsaw (1962).
10. F. Erdogan and G. D. Gupta, On the numerical solution of singular integral equations. *Quart. App. Math.* 525–534 (1972).
11. R. J. Asaro and D. M. Barnett, The non-uniform transformation strain problem for an anisotropic ellipsoidal inclusion. *J. Mech. Phys. Solids* **13**, 77–83 (1975).
12. D. A. Simons, Boundary-layer analysis of propagating mode II cracks in porous elastic media. *Jour. Mech. Phys. Solids*, **25**, 99–115 (1977).
13. J. H. Weiner, Thermoelastic dissipation due to high-speed dislocations. *J. Appl. Phys.* **29**(9), 1305–1307 (1958).

APPENDIX 1

It is possible to derive the complete stress field of the moving line source and compare with the solution of eqns (12), (13c), obtained by means of eqn (6) on the plane of motion of the source. First, observe that in deducing eqn (6), we simply added the effects of a sequence of stationary source problems, all of them having displacement fields expressible as the gradient of a scalar function.† Assume that u_i, the displacement field of the moving source, preserves this property: then we have shown (Chap. 3 of [2]) that the diffusion process is governed by an uncoupled diffusion equation

$$cp_{,kk} - \frac{\partial p}{\partial t} = -\frac{\gamma^F}{\rho_0 \kappa}, \quad \gamma^F = q\delta(x_2)\delta(x_1 - Vt). \tag{A1.1}$$

This can be converted to the moving co-ordinate system ($x_2 = y$, $x_1 - Vt = x$) to get

$$p_{,xx} + p_{,yy} + \left(\frac{V}{c}\right) p_{,x} = \frac{-q\delta(x)\delta(y)}{\rho_0 \kappa}. \tag{A1.2}$$

We recognise that $p = \hat{p}e^{-Vx/2c}$ is a natural trial solution which will remove the x-bias and we find that $\hat{p}$ then satisfies a Bessel equation in the radial co-ordinate with a source term at the origin. The solution is thereby found to be

$$p = \frac{q}{2\pi\rho_0\kappa} e^{-Vx/2c} K_0(R), \quad R = V(x^2 + y^2)^{1/2}/2c, \tag{A1.3}$$

where $K_0(z)$ is the zeroeth order Bessel function of the second kind[4]. This solution has been given by Carslaw and Jaegar ([8], Section 10.7) and by Nowacki ([9], Section 7.4), but in a much less transparent fashion.

We introduce the potential ϕ by $u_i = \phi_{,i}$ and find (eqn (15) in Chap. 3 of [2]) that

$$\nabla^2\phi = \phi_{,xx} + \phi_{,yy} = \eta p/G. \tag{A1.4}$$

It is convenient to solve for the function $\phi_{,x}$ since eqn (A1.2) shows that

$$\nabla^2\left[\phi_{,x} + \frac{\eta c}{GV} p\right] \simeq \frac{\eta c}{GV}\left[\frac{-q\delta(x)\delta(y)}{\rho_0\kappa}\right] \tag{A1.5}$$

We observe that eqn (A1.5) has the standard Green function solution of the harmonic operator, in the plane and when we substitute for p from eqn (A1.3) we obtain the final solution (defining $r = (x^2 + y^2)^{1/2}$).

$$\phi_{,x} \simeq \frac{-\eta c}{GV}\left(\frac{q}{2\pi\rho_0\kappa}\right)[e^{-Vx/2c}K_0(R) + \ln r]. \tag{A1.6}$$

Now it is also easy to show (combine eqns (12), (15) in Chap. 3 of [2]) that

$$\begin{Bmatrix}\sigma_{xx}\\ \sigma_{yy}\\ \sigma_{xy}\end{Bmatrix} = -2G\begin{Bmatrix}\phi_{,yy}\\ \phi_{,xx}\\ -\phi_{,xy}\end{Bmatrix}. \tag{A1.7}$$

By noting that $K_0'(R) = -K_1(R)$ we first obtain

$$\sigma_{yy} = \frac{-\eta q}{2\pi\rho_0\kappa}\left[e^{-Vx/2c}\left(K_0(R) + \frac{x}{r}K_1(R)\right) - \frac{x}{r}\left(\frac{1}{R}\right)\right] \tag{A1.8}$$

$$\sigma_{xy} = \frac{\eta q}{2\pi\rho_0\kappa}\left(\frac{y}{r}\right)\left[e^{-Vx/2c}K_1(R) - \frac{1}{R}\right] \tag{A1.9}$$

†This class of problems is discussed in Chap. 3 of [2], where a proof is given.

and then, after reverting to eqn (A1.4) for $\nabla^2\phi$, we deduce

$$\sigma_{xx} = \frac{-\eta q}{2\pi\rho_0\kappa}\left[e^{-Vx/2c}\left(K_0(R) - \frac{x}{r}K_1(R)\right) + \left(\frac{x}{r}\right)\frac{1}{R}\right] \tag{A1.10}$$

By setting $y = 0$, we obtain perfect agreement with eqns (12), (13c) and (13d).

APPENDIX 2

The method of polynomial interpolation

We are interested in the solution of singular integral equations of the kind in eqn (20) by means of interpolation functions, as suggested by eqn (21). We are anxious to identify the special functions (if any) which are appropriate to the domain in question, to the singularity in the kernel and to the expected singularity in the unknowns, $\mu(z)$ for instance. The idea can be consolidated by means of an example: let the domain be the internal interval $(-1, +1)$ and let the kernel have an $(x-z)^{-1}$ singularity. This class of problems includes the fault problems solved in the main text.

First, note the integral relations given by Abramowitz and Stegun [4, p. 785], namely† (PV denoting a principal value integral)

$$\frac{1}{\pi}PV\int_{-1}^{+1}\frac{T_n(t)\,dt}{(t-x)\sqrt{(1-t^2)}} = U_{n-1}(x), \quad n>0 \tag{A2.1}$$

$$\frac{1}{\pi}PV\int_{-1}^{+1}\frac{U_{n-1}(t)\sqrt{(1-t^2)}\,dt}{(t-x)} = -T_n(x), \quad n>0. \tag{A2.2}$$

The special functions in use here are the Gauss–Chebyshev polynomials, most conveniently defined as

$$T_n(x) = \cos n\theta, \quad U_n(x) = \frac{\sin(n+1)\theta}{\sin\theta}, \quad x \equiv \cos\theta \tag{A2.3}$$

These polynomials are conventionally used in integration formulae for the domain $(-1, +1)$, for instance [4, 25.4.38]

$$\frac{1}{\pi}\int_{-1}^{+1}\frac{g(t)\,dt}{\sqrt{(1-t^2)}} = \sum_{k=1}^{M}\frac{g(t_k)}{M}, \quad t_k = \cos\frac{\pi(2k-1)}{2M} \tag{A2.4}$$

where the nodal points t_k are the zeroes for the polynomials of the first kind $T_M(t)$.

Suppose that the integral equation is of the special kind (e.g. eqn (23))

$$\sigma(x) = \frac{C}{\pi}\int_{-1}^{+1}\frac{F(t)}{\sqrt{(1-t^2)}}[(t-x)^{-1} + k(x,t)]\,dt, \quad -1 \le x \le 1 \tag{A2.5}$$

where $k(x, t)$ is a bounded smooth kernel (see [7] for more rigorous statements) and $\mu(t) = F(t)/\sqrt{(1-t^2)}$ might be the dislocation density of the main text. The idea is that we shall approximate the unknown function $F(t)$ by a series of the Chebyshev polynomials

$$F(t) \simeq \sum_{n=1}^{N} B_n T_n(t). \tag{A2.6}$$

The integral equation then takes the form

$$\sum_{k=1}^{M} k(x, t_k)F(t_k) + M\sum_{n=1}^{N} B_n U_{n-1}(x) = M\sigma(x)/C\pi. \tag{A2.7}$$

Now the integral equation may be reduced to linear algebraic equations for the unknowns B_n (analogous to eqns (22) in the main text), namely

$$\sum_{n=1}^{N}\left[\sum_{k=1}^{M} k(x_i, t_k)T_n(t_k) + MU_{n-1}(x_i)\right]B_n = M\sigma(x_i)/C\pi, \quad i = 1, \ldots N. \tag{A2.8}$$

Now the x_i seem to be perfectly arbitrary and should be chosen to give well-conditioned matrices: the procedure in eqn (A2.8) is one of simple collocation.

A major contribution to the scheme just envisioned was made by Erdogan and Gupta[10]. We notice that we did not employ the integration formula (A2.4) but rather used (A2.1) on the singular part of the integral equation: it would be convenient if (A2.4) were valid also for the singular part even if only for special $x = x_r$. This is exactly what they proved.

The formula established by Erdogan and Gupta[10] was

$$U_{n-1}(x_r) = \sum_{k=1}^{M}\frac{T_n(t_k)}{M(t_k - x_r)}, \quad x_r = \cos\left(\frac{\pi r}{M+1}\right) \tag{A2.9}$$

which means that the integration formula (A2.4) also holds in (A2.1) if the evaluation points x_r are the zero points of

†Note that a special case, $n = 0$, is $\int_{-1}^{+1} dt/(t-x)\sqrt{(1-t^2)} = 0$ which is useful in extracting the solution of the homogeneous singular integral equation.

$U_{M-1}(x)$. Now eqn (A2.7) again simplifies considerably to a very workable form

$$\sum_{k=1}^{M} [(t_d - x_r)^{-1} + k(x_r, t_k)]F(t_k) = M\sigma(x_r)/C\pi, \quad r = 1, \ldots, M-1. \tag{A2.10}$$

This eqn (A2.10) is preferable to eqn (A2.8) since it makes little reference to the polynomials used except through their zero-points, t_k and x_r. In general, we need an extra condition on the $F(t_k)$ to close the system in (A2.10): typically, this is phrased as a specification of the net entrapped dislocation in the fault, say b_F in magnitude (typically $b_F = 0$), hence

$$\int_{-1}^{+1} \frac{F(t)}{\sqrt{(1-t^2)}}\,dt \equiv b_F \simeq \sum_{k=1}^{M} \frac{F(t_k)}{M}. \tag{A2.11}$$

Thus the interior fault, transformable onto $(-1, +1)$, is very tractable. Even if the fault closes smoothly, we can go through entirely analogous procedures with $(1-t^2)^{1/2}$, instead of $(1-t^2)^{-1/2}$, and still get a simple matrix equation like (A2.10), as discussed by Erdogan and Gupta[10]. There is a striking similarity between the integration formulae (A2.1, A2.2) and the result given in [11]: they found that the stress-field of an inclusion, that is an anomalous internal region undergoing a polynomial transformation strain, is also expressible as a polynomial of the same order. Formulae (A2.1, A2.2) are no more than the stress fields of a flat crack-like inclusion on the line of the crack where the strain is an intense shear, uniform in the thickness direction but given by a polynomial $T_n(t)$ or $U_{n-1}(t)$ along its length.

APPENDIX 3

Fourier transform technique

An alternative scheme for deriving the influence functions of moving singularities (in particular those producing plane deformation conditions) is exemplified by the following outline. First we write the governing equations for plane strain of a fluid-saturated porous medium, e.g. as in [1, 3], namely (with $\nabla^2 \equiv \partial^2/\partial x^2 + \partial^2/\partial y^2$)

$$\nabla^2(\sigma_{xx} + \sigma_{yy} + 2\eta p) = 0 \tag{A3.1}$$

$$\left[c\nabla^2 - \frac{\partial}{\partial t}\right]\left(\sigma_{xx} + \sigma_{yy} + \frac{2\eta(1-\nu)}{(\nu_u - \nu)}p\right) = 0 \tag{A3.2}$$

$$\frac{\partial \sigma_{xx}}{\partial x} + \frac{\partial \sigma_{xy}}{\partial y} = 0 = \frac{\partial \sigma_{xy}}{\partial x} + \frac{\partial \sigma_{yy}}{\partial y}. \tag{A3.3}$$

Since we are concerned with steady-state motion (with velocity V) of the singularity, any of the four unknown variables σ_{xx}, σ_{xy}, σ_{yy} or p, generically denoted by function $f = f(x, y, t)$, really depends only on y and $X \equiv x - Vt$, so the function becomes $f \equiv f(X, y)$ and eqn (A3.2) can be reduced (since $\sigma_{xx} \equiv \sigma_{XX}$, $\sigma_{xy} \equiv \sigma_{Xy}$) to

$$\left[\kappa\nabla^2 + V\frac{\partial}{\partial X}\right]\left(\sigma_{xx} + \sigma_{yy} + \frac{2\eta(1-\nu)}{(\nu_u - \nu)}p\right) = 0. \tag{A3.2bis}$$

We now perform a Fourier transformation with respect to the variable X, defined by

$$\tilde{f}(k, y) \equiv \int_{-\infty}^{\infty} f(X, y)\,e^{-ikX}\,dX \tag{A3.4}$$

We rewrite the governing equations in terms of the transformed field variables,

$$\left[\frac{\partial^2}{\partial y^2} - k^2\right](\tilde{\sigma}_{XX} + \tilde{\sigma}_{yy} + 2\eta\tilde{p}) = 0 \tag{A3.5}$$

$$\left[\frac{\partial^2}{\partial y^2} - k^2 - ikV/c\right]\left(\tilde{\sigma}_{XX} + \tilde{\sigma}_{yy} + \frac{2\eta(1-\nu)}{(\nu_u - \nu)}\tilde{p}\right) = 0 \tag{A3.6}$$

while performing a little manipulation to make the equilibrium eqns (A3.3) more transparent,

$$-ik(\tilde{\sigma}_{yy} - \tilde{\sigma}_{XX})/2 + \partial\tilde{\sigma}_{Xy}/\partial y = -ik(\tilde{\sigma}_{XX} + \tilde{\sigma}_{yy})/2 \tag{A3.7}_1$$

$$2ik\tilde{\sigma}_{Xy} + \partial[\tilde{\sigma}_{yy} - \tilde{\sigma}_{XX}]/\partial y = -\partial[\tilde{\sigma}_{yy} + \tilde{\sigma}_{XX}]/\partial y \tag{A3.7}_2$$

Obviously, the latter can now be reduced to

$$\left[\frac{\partial^2}{\partial y^2} - k^2\right]\tilde{\sigma}_{Xy} = -ik\frac{\partial}{\partial y}(\tilde{\sigma}_{yy} + \tilde{\sigma}_{XX}) \tag{A3.8}_1$$

$$\left[\frac{\partial^2}{\partial y^2} - k^2\right](\tilde{\sigma}_{yy} - \tilde{\sigma}_{XX}) = -\left[\frac{\partial^2}{\partial y^2} - k^2\right](\tilde{\sigma}_{yy} + \tilde{\sigma}_{XX}) \tag{A3.8}_2$$

It is now completely straightforward to write the general solutions to the eqns (A3.5), (A3.6), (A3.8), thereby determining the transforms of the field variables: the homogeneous solutions (adhering to convention in [3]) take the form $2(1-\nu_u)A(k)\,e^{\pm my}/(1-\nu)$ in eqn (A3.5) and $-2(1-\nu_u)B(k)\,e^{\pm ny}/(\nu_u - \nu)$ in eqn (A3.6) while the homogeneous solutions in eqns (A3.8) are also of the form $\tilde{\sigma}_{yy} - \tilde{\sigma}_{XX} = 2C(k)\,e^{\pm my}$ (multiplied by $(\mp ik/m)$ for $\tilde{\sigma}_{Xy}$) where $m^2(k) \equiv k^2$ and $n^2(k) \equiv k^2 - ikV/c$.

The particular solutions of eqn (A3.8) are then simple to determine and the rationalized results are

$$-n\tilde{p} = (\nu_u - \nu)A(k)\,e^{\pm my}/(1-\nu) - B(k)\,e^{\pm ny} \tag{A3.9}$$

$$(\tilde{\sigma}_{XX} + \tilde{\sigma}_{yy}) = 2A(k)\,e^{\pm my} + 2B(k)\,e^{\pm ny} \tag{A3.10}$$

$$(\tilde{\sigma}_{yy} - \tilde{\sigma}_{xx}) = 2[C(k) \mp mAy]\,e^{\pm my} + \left[\frac{k^2+n^2}{k^2-n^2}\right] B\,e^{\pm ny} \tag{A3.11}$$

$$\tilde{\sigma}_{xy} = -\left[\mp\frac{ikC}{m} + ikAy\right] e^{\pm my} \pm \left[\frac{2ikn}{k^2-n^2}\right] B\,e^{\pm ny} \tag{A3.12}$$

For our purposes it will be adequate to choose the solution which vanishes as $y \to +\infty$, thus we shall adopt the solution involving e^{-my}, e^{-ny}.

To apply the transform technique directly to the problems of moving singularities considered in the body of the paper was found not to be a simple task.† Instead, let us adopt the attitude that Figs. 4(a, b) provide us with values of the field variables on the trajectory of motion $y = 0$ and establish how much progress we can make on the basis of that assumption. For example, consider the "gliding" dislocation: for this, on $y = 0$, $p = 0 = \sigma_{yy}$, so that eqns (A3.9–A3.11) imply $A = -B(1-\nu)/(\nu_u - \nu)$ and $C = B[(1+\nu-2\nu_u)k^2 - (1-\nu)n^2]/[(\nu_u - \nu)(k^2 - n^2)]$. Thus, only $B(k)$ needs to be determined and we note that, on $y = 0$, eqn (A3.12) implies

$$\tilde{\sigma}_{Xy} = -ikB[(1+\nu-2\nu_u) - (1-\nu)n^2 + 2(\nu_u - \nu)mn]/[(\nu_u - \nu)m(k^2 - n^2)] \equiv Bg(k);$$

however,

$$\sigma_{Xy}(y=0) = Gb\left[1 - \frac{\nu_u - \nu}{1-\nu} g_1\left(\frac{VX}{4c}\right)\right]/[2\pi(1-\nu_u)X] \equiv \tau(X),$$

where g_1 is plotted in Fig. 4(a). Clearly, then, $B(k) = \tilde{\tau}(k)/g(k)$ and all of the unknown functions $A(k)$, $B(k)$, $C(k)$ are determined.

Similarly, for the "climbing" dislocations we know that $\tilde{\sigma}_{Xy}(y=0) = 0$ and both p and σ_{yy} are given on $y = 0$ by eqns. (16c), (19) in the main text, so that $A(k)$, $B(k)$ and $C(k)$ are again formally determined. Then eqns (A3.9)–(A3.12) give the complete field solution as a convolution of our known influence functions (eqns (14), (19)) off the real axis $y = 0$; the associated computations appear to be inescapably numerical.‡ These have not yet been performed, partly because we hope that we may be able to find some convenient characteristic of the functions to be transformed (thus avoiding the apparently innate complication of transforms associated with dislocation and fault problems, e.g. see [3] also): the more immediate reason for postponing the calculations was, however, simply that the complete version of influence functions is not needed for most of the fracture simulation of immediate interest to us.

†The technique has been employed by Weiner[13] (prompted by the convenience of the Parseval theorem) to compute energy dissipation due to moving dislocations in a thermoelastic medium. However, he makes assumptions which avoid rigorously solving the coupled elasto-diffusion equations and his results are not useful here.

‡An exception, again, seems to be the steady-state source problem. However, the difficulty of performing Wiener–Hopf separation of analytic functions[3] is avoided and adept artists of transform inversion are encouraged to try their hand.